# ChAdOx1 nCoV-19 protection against SARS-CoV-2 in rhesus macaque and ferret challenge models

**Teresa Lambe**
University of Oxford https://orcid.org/0000-0001-7711-897X
**Alexandra Spencer**
University of Oxford https://orcid.org/0000-0001-7958-6961
**Kelly Thomas**
National Infection Service, Public Health England https://orcid.org/0000-0002-0348-654X
**Stephen Thomas**
Public Health England
**Andrew White**
Public Health England https://orcid.org/0000-0001-9481-0079
**Holly Humphries**
Public Health England https://orcid.org/0000-0003-2576-8502
**Daniel Wright**
University of Oxford https://orcid.org/0000-0002-8114-1838
**Nazia Thakur**
The Pirbright Institute https://orcid.org/0000-0002-4450-5911
**Carina Conceicao**
University of Edinburgh
**Leonie Alden**
Public Health England
**Lauren Allen**
Public Health England
**Marilyn Aram**
Public Health England
**Kevin Bewley**
Public Health England https://orcid.org/0000-0002-9078-6734
**Emily Brunt**
Public Health England
**Phillip Brown**
Public Health England https://orcid.org/0000-0001-6367-6495
**Breeze Cavell**
National Infection Service, Public Health England https://orcid.org/0000-0001-9897-1590
**Rebecca Cobb**

Public Health England
**Susan Fotheringham**
Public Health England
**Ciaran Gilbride**
University of Oxford
**Debbie Harris**
Public Health England
**Catherine Ho**
National Infection Service, Public Health England
**Laura Hunter**
National Infection Service, Public Health England
**Chelsea Kennard**
National Infection Service, Public Health England
**Stephanie Leung**
National Infection Service, Public Health England
**V Lucas**
Public Health England
**Didier Ngabo**
National Infection Service, Public Health England https://orcid.org/0000-0003-1818-1439
**Kathryn Ryan**
Public Health England https://orcid.org/0000-0001-8608-1144
**Hannah Sharpe**
University of Oxford
**Charlotte Sarfas**
Public Health England
**Laura Sibley**
Public Health England
**Gillian Slack**
National Infection Service, Public Health England
**Marta Ulaszewska**
University of Oxford
**Nadina wand**
Public Health England https://orcid.org/0000-0002-5518-4367
**Nathan Wiblin**
Public Health England
**Fergus Gleeson**
University of Oxford
**Dalan Bailey**
The Pirbright Instiute

**Sally Sharpe**
Public Health England
**Sue Charlton**
Public Health England
**Francisco Salguero**
Public Health England
**Miles Carroll**
Public Health England
**Sarah Gilbert** (✉ sarah.gilbert@ndm.ox.ac.uk)
University of Oxford https://orcid.org/0000-0002-6823-9750

---

**Article**

**Keywords:** SARS-CoV-2, vaccines, immune profiling

**Posted Date:** January 13th, 2021

**DOI:** https://doi.org/10.21203/rs.3.rs-133970/v1



---

**Version of Record:** A version of this preprint was published at Communications Biology on July 26th, 2021. See the published version at https://doi.org/10.1038/s42003-021-02443-0.

# Abstract

Vaccines against SARS-CoV-2 are urgently required. Here we report detailed immune profiling after ChAdOx1 nCoV-19 (AZD1222) and subsequent challenge in two animal models of SARS-CoV-2 mediated disease. We demonstrate in rhesus macaques the lung pathology caused by SARS-CoV-2 mediated pneumonia is reduced by prior vaccination with ChAdOx1 nCoV-19 which induced neutralising antibody responses after a single intramuscular administration. In a second animal model, ferrets, ChAdOx1 nCoV-19 reduced both virus shedding and lung pathology. Antibody titers were boosted by a second dose. Data from these challenge models and the detailed immune profiling, support the continued clinical evaluation of ChAdOx1 nCoV-19.


# Introduction

In response to the COVID-19 pandemic, multiple candidate vaccines have entered preclinical and clinical development, and clinical efficacy has now been demonstrated for two vaccines (*1, 2*). Inactivated (*3, 4*), adenoviral-vectored (*5, 6*) RNA (*7*) and DNA vaccines (*8, 9*) have demonstrated protection against SARS-CoV-2 challenge in rhesus macaques, and SARS-CoV-2 infection has been shown to protect against rechallenge in this species (*10, 11*). Non-human primate challenge studies following vaccination with candidate vaccines are principally used to assess vaccine safety, ruling out evidence of vaccine enhanced disease after vaccination and challenge. Here we report on studies in two different animal models following vaccination with ChAdOx1 nCoV-19 (AZD1222) and subsequent SARS-CoV-2 challenge. In rhesus macaques we show, using computerised tomography (CT) scanning, that the changes in the lungs induced after SARS-CoV-2 challenge are similar to the changes in human lung tissue during COVID-19, and can be prevented by intramuscular vaccination with ChAdOx1 nCoV-19. Importantly it has been demonstrated in the ferret model system that vaccine enhanced disease can be transiently induced by a formalin inactivated alum-adjuvanted SARS-CoV-2 vaccine (FIV), resulting in increased lung pathology after vaccination and challenge when compared to unvaccinated animals (*12*). Here we demonstrate that in the same model, lung pathology is reduced following ChAdOx1 nCoV-19 vaccination and challenge when compared to animals vaccinated with vaccine expressing an irrelevant antigen (green fluorescent protein; GFP).

Importantly, this work demonstrates both safety and a reduction in disease pathology in two animal models using a new methodology to detect disease. Further evidence of a Th1 bias after vaccination with ChAdOx1 nCoV-19 is demonstrated and the immune response post vaccination with ChAdOx1 nCoV-19 and after challenge with SAS CoV-2 is described.

# Results

**Immune response to ChAdOx1 nCoV-19 vaccination in rhesus macaques and ferrets**.

ChAdOx1 nCoV-19 is a replication-deficient simian adenoviral vector expressing a codon-optimised full-length SARS-CoV-2 spike protein that has been shown to prevent SARS-CoV-2 pneumonia in rhesus macaques at a dose of 2.5 x $10^{10}$ vp (*6*) and is immunogenic with an acceptable safety profile in humans at a dose of 5 x $10^{10}$ vp (*13*). Here, six adult rhesus macaques (three male, three female) were vaccinated with a single dose of 2.5 x $10^{10}$ vp, with an equivalent control group receiving saline injections. Humoral immunogenicity was assessed at 14 and 27 days after vaccination by ELISA, with IgG (Fig. 1A), IgM and IgA (Fig. S1A) spike-specific antibodies induced in all the vaccinated animals. Neutralising antibodies were assessed in a $PRNT_{50}$ assay, determining the antibody titre required for a 50% reduction in viral plaque formation in susceptible cells. All six vaccinated animals produced neutralising antibodies with a median titre of 74.5 (sd 76.6) at day 14 and 95 (sd 131) at day 27. (Fig. 1A). Neutralising antibodies were also assessed in a pseudo neutralization assay (Fig. 1A), with a correlation ($r^2$=0.4032, p=0.0265) between the two neutralisation assays (Fig. S1A right).

In all ferrets immunised with a single dose of 2.5 x $10^{10}$ vp ChAdOx1 nCoV-19, spike-specific IgG (Fig. 1B), IgM and IgA (Fig. S1B) antibodies were increased relative to animals vaccinated with control ChAdOx1 GFP vector, expressing green fluorescent protein as the vaccine antigen. $PRNT_{50}$ titres reached 1118 (sd 478) at day 14 and 1708 (sd 809) at day 28 (median of 11 animals) (Fig. 1B). In six ferrets receiving a second vaccine dose at day 28, titres increased from 1379 (sd 699) at day 28 to 3867 (sd 1645) at day 35 (median of 6 animals). These titres were not significantly higher than a single dose vaccination (Fig. 1B). Consistent with NHP antibody responses, pseudo neutralisation assays showed similar high titres post-vaccination, (Fig. 1B) with strong correlation ($r^2$=0.6714 p<0.0001) between neutralisation assays (Fig. S1B).

T cell responses to SARS-CoV-2 spike were also assessed by interferon-gamma ELISpot in both rhesus macaques and ferrets. A significant increase in the total spike-specific T cell response was observed at day 14 in rhesus macaques (Fig. 2A). Across the peptide pools spanning the spike protein T cell responses were measured against all regions (Fig. 2A); however responses were typically higher to S1 peptide pools when compared to S2, (Fig. 2A). Measurement of cytokine production in the supernatant of PMBCs stimulated with spike peptides spanning the dominant S1 region showed a log increase in IL2 levels in vaccinated animals when compared to PBS control animals (Fig. S2A). In addition, an increase in IFNg was measured. No change in IL1b, IL8, IL6 or IL10 was measured between ChAdOx1 nCoV-19 vaccinated animals and PBS control animals. Simultaneous measurement of IFNg, IL5 or IL13 by FLUROSpot assay on day 27 rhesus macaque PBMCs, stimulated with spike peptides, demonstrated Th1 bias of the antigen specific response with a higher number of antigen specific IFNg producing cells observed, compared to cells producing either IL5 or IL13. (Fig. S2B).

A statistically significant (p=0.001) increase in spike specific T cells was observed in ferrets from day 14 onwards when compared to the day of vaccination (Fig. 2B), and a small but non-significant increase in IFNg producing T cells was observed after boosting. Mapping of T cell responses across peptides spanning the spike protein, showed responses to all peptide pools, which were predominantly directed

against the S1 peptide pools (pool 1 and pool 2) (Fig. 2B), with proportional responses to individual pools in each animal not changing over time (Fig. S3A). At day 28 post-vaccination, antigen specific $IFNg^+$ $CD8^+$ T cell responses were detected by flow cytometry (Fig. 2B). No statistically significant difference in $IFNg^+$, $TNFa^+$ or $IL4^+$ $CD4^+$ T cells was observed between ChAdOx1 nCoV-19 and ChAdOx1-GFP vaccinated animals a on day 28 (Fig. 2B) (data not shown). Comparison of IFNg detected by ELISpot or ICS demonstrated that $CD8^+$ T cells were the predominant population producing IFNg at day 28 post-vaccination (Fig. 2B).

## CT assessment of SARS-CoV-2 disease in vaccinated and non-vaccinated rhesus macaques after SARS-CoV-2 challenge.

Twenty seven days after vaccination all twelve rhesus macaques were challenged with a total of $5 \times 10^6$ pfu SARS-CoV-2 administered via both intratracheal and intranasal routes. CT scans were performed on all animals 15 days prior to challenge and on day 5 after challenge. Two animals per group were euthanized at day 7 for necropsy, and CT scans were performed again on day 12 in the remaining animals. Representative examples of the CT scans are shown in (Fig. 3A and S4A.). A scoring system (Table S1) was used to quantitate disease pattern and distribution (Fig. S4B and Table S2) (Supplementary Methods) which was combined to produce a total score (Fig. 3A) (*14*). The CT scans confirm that five days after direct instillation of SARS-CoV-2 into the trachea and nose, lung tissue became infected resulting in pathological findings similar to mild clinical cases of human COVID-19 (*15*). These changes were seen in four out of six saline control and two out of six ChAdOx1 nCoV-19 vaccinated macaques, with reduced disease scores in the two vaccinated animals who demonstrated pulmonary changes (Fig. 3A).

As in human disease, higher incidence of abnormalities in the lungs was observed in males than in females. Some abnormalities were detected in all male animals on either day 5 or day 12 post challenge, but only 50% of females (Table S1). Where abnormalities were reported they were at low levels with less than 25% of the lung involved, indicating that rhesus macaques experience mild disease in this challenge model similar to mild clinical cases of human disease (Fig. S4C). There were fewer abnormal findings in vaccinated than control animals at day 5 post challenge, with equivalent amounts at day 12 (Fig. S4C). Systemic monitoring of animal health showed significantly more weight loss in control animals compared to ChAdOx1 nCoV-19 vaccinated animals ($p=0.0108$) (Fig. S4D). Over the entire post-challenge period, no statistically significant difference in body temperature between groups was observed, however at day 1 post challenge control animals had a higher median body temperature (39.4, sd 0.423) compared to vaccinees (median 38.8, sd 0.480) (Fig. S4E). Similarly, a small increase in body temperature in controls animals (median 39.050, sd 0.204) compared to ChAdOx1 nCoV-19 vaccinated animals (38.45, sd 0.383) was also observed at day 3 post challenge.

## Detection of viral RNA and histopathology following challenge of rhesus macaques

Bronchoalveolar lavage was performed at necropsy in two animals per group on days 7, 13 and 14 post-challenge. Viral RNA was only detected in bronchoalveolar lavage fluid (BALF) from control animals (Fig. 3B). Viral RNA was also quantitated in nasal wash samples and throat swabs with similar results in both groups (Fig. 3B).

Viral RNA was detected in staining of lung tissue sections in both control animals on day 7 post-challenge and three out of four control animals on day 13/14, but only one vaccinated animal, on day 7 (Fig. 3C). Lesions consistent with infection with SARS-CoV-2 were observed in the lungs of animals from both the control and vaccinated groups (Fig. 3D), with a considerably greater severity in one of the control animals. These lesions included diffuse alveolar damage, alveolar hyperplasia, perivascular and peribronchiolar lymphoid infiltrates and bronchial/bronchiolar necrosis and exudates (Fig. 3D). No significant changes were observed in any other tissues examined. At 13/14 days post-challenge, multifocal areas of lung pathology, as described at 7 days post-challenge, together with signs of lesion resolution, were noted at reduced severity in three out of the four control animals; in the remaining animal, lesion severity had not reduced. Minimal lesions were also noted in three out of four vaccinated animals; however, in one animal, mild, multifocal interstitial pneumonia and perivascular cuffing was observed.

### Detection of virus and histopathology following challenge of ferrets

Ferrets were challenged with 5 x $10^6$ pfu SARS-CoV-2 administered intranasally 28 days after the last vaccination, and the duration of challenge was 14 days. Challenges were staggered and took place for these groups initially (ChAdOx1 nCoV-19 and ChAdOx1 GFP prime only) followed by two further groups (ChAdOx1 nCoV-19 and ChAdOx1 GFP prime boost). Viral RNA was detected in all groups in nasal wash samples two days after challenge, with reductions in the ChAdOx1 nCoV-19 vaccinated groups by day 4 and all vaccinated animals except for one were negative at day 6 (Fig. 4A). Viral RNA in nasal washes over the total challenge period tended to be lower in the prime boost group than prime only (Fig. 4A). In contrast, in the ChAdOx1 GFP control groups (after one or two doses of ChAdOx1 GFP) the viral RNA in the nasal washes remained above the limit of quantification until day 6, (Fig. 4A). Minimal viral RNA was detected in throat swabs or BALF samples in any of the groups (Fig S5A), with no virus above baseline detected in the lung of any animal (data not shown).

Histopathology was performed on two animals per group at day 6/7 post infection and the remainder at days 13/14, with scores summarized in Fig. 4B and detailed findings included in the supplementary information. Animals vaccinated with one dose of ChAdOx1 nCoV-19 did not show any remarkable change in the lungs. On day 6/7 days post-infection in the group vaccinated with only one dose of ChAdOx1 GFP, one animal had mild lesions compatible with subacute bronchopneumonia and the other had occasional minimal bronchiolar infiltrates. In ferrets receiving one dose of ChAdOx1 GFP, histopathological changes at 13/14 days post-infection were reduced compared to 6 days post-infection. Minimal changes were observed in the lungs of animals receiving 2 doses of ChAdOx1 nCoV-19 at either 6 or 13/14 days post-infection, and a significant increase was measured in the histology score (minimal

to mild changes) in the group receiving 2 doses of ChAdOx1 GFP when compared to the two dose ChAdOx1 nCoV-19 group.

### Anamnestic responses following challenge

Responses were assessed in a virus $IC_{50}$ neutralisation assay showing an increased neutralisation titre from day 3 post challenge to day 7 or day 13/14 in vaccinated non-human primates, and days 7 to 13/14 in PBS controls (Fig. 5A left). Antigen-specific cellular immune responses were measured in PBMCs stimulated with overlapping 15-mer SARS-CoV-2 spike protein peptide pools, using an *ex vivo* IFN-g ELISpot assay and also showed an increase in antigen specific responses post-challenge in both ChAdOx1 nCoV-19 vaccinated and PBS control rhesus macaques after day 3 (Fig. 5A right). The median response in ChAdOx1 nCoV-19 vaccinated animals was higher than that measured in the PBS control animals on day 7 and day 13/14 post-challenge (Fig. 5A right).

Immunophenotyping flow cytometry assays were applied to whole blood samples collected immediately prior to (27 days after ChAdOx1 nCoV-19 vaccination), and at days three, seven and 13-14 after SARS-CoV-2 challenge to explore changes in the composition and activation status of the cellular immune compartment (Fig. 5B). T cell activation status was assessed by expression of the class II major histocompatibility antigen, HLA-DR, and the immune checkpoint signaling receptor PD-1. Transient increases in the number of $CD4^+$ and $CD8^+$ T cells expressing PD-1 were observed following SARS-CoV-2 infection in both ChAdOx1 nCoV-19 and PBS vaccinated animals (Fig. 5B). However, the number of activated HLA-DR expressing $CD4^+$ T cells was significantly higher in ChAdOx1 nCoV-19 animals three days after SARS-CoV-2 challenge ($p = 0.004$), indicating that ChAdOx1 nCoV-19 vaccination had advanced the kinetics of the adaptive T cell mediated response to infection. Similarly, the quantification of classical ($CD14^+CD16^-$), non-classical ($CD14^-CD16^+$) and intermediate ($CD14^+CD16^+$) monocyte populations revealed significant increases in immunomodulatory populations ($p=0.031$ intermediate; $p=0.031$ non-classical) in vaccinated animals suggesting that heightened early pro-inflammatory responses had been facilitated by the vaccination regimen (Fig. 5C).

In ferrets, neutralising antibodies did not dramatically increase in ChAdOx1 nCoV-19 vaccinated animals following SARS CoV-2 challenge, with both groups having similar titres of neutralising antibodies by the end of the study (Fig. 5D). In ChAdOx1 nCoV-19 vaccinated animals, the IgG antibody titres on the day of challenge, measured by ELISA, neutralisation or pseudo neutralisation assay, inversely correlated with the peak level of viraemia measured in each animal (Fig. 5E). There was no relationship between IFNg ELISpot and peak viraemia. Overall the data would suggest that vaccine induced protection in ferrets was not associated with the level of spike specific T cells measured in these assays, but was associated with the humoral response to SARS-CoV-2 spike protein.

# Discussion

A safe and effective vaccine is expected to be an essential requirement to effectively control the COVID-19 pandemic. Early development of a vaccine against Feline Infectious Peritonitis, which is also caused by a coronavirus, resulted in enhanced disease in vaccinated and then challenged animals (*16*), a phenomenon also seen in early development of vaccines against SARS-CoV-1(*17, 18*). Vaccine enhanced disease results in an increase in disease severity when vaccinated subjects are subsequently exposed or challenged with natural virus. Immunopathology in coronavirus vaccinated and challenged animals has been associated with increased levels of the Th2 cytokines IL5 and IL13 and altered ratios of IgG antibody subclasses (*8,9,11-13,15*). This is similar to the vaccine enhanced disease observed with early vaccine development against respiratory syncytial virus (RSV); pathology was associated with relatively high titers of non-neutralising antibodies, a role for neutrophils, eosinophils and a predominantly a Th2-biased response was described (*19-23*).

Preclinical studies of vaccines against SARS CoV-2 must therefore determine whether enhanced disease occurs in vaccinated animals once exposed to SARS-CoV-2 virus. Multiple studies of SARS-CoV-2 vaccines (*3-8*) have now been conducted in rhesus macaques without demonstrating enhanced disease. Using CT scanning, we show that the lung pathology associated with infection with $5x10^6$ pfu of SARS-CoV-2 in rhesus macaques closely mirrors that seen in humans with mild pneumonia caused by COVID-19, and is reduced in animals vaccinated with a single dose of ChAdOx1 nCoV-19 during the first week post-infection. Histopathology performed on the lung tissues also indicated that the lesions observed in vaccinated animals are less severe than in controls at 7 days post-challenge, but also at 13/14 days post-challenge. The presence of viral RNA (using a probe that does not allow determination of viral replication) by ISH is also less frequent in vaccinated animals.

We demonstrate in the ferret model that virus shedding early after challenge with $5x10^6$ pfu of SARS-CoV-2 was reduced in ChAdOx1 nCoV-19 vaccinated animals. A second vaccination with ChAdOx1 nCoV-19 transiently increased antibody titres in ferrets, which showed a negative correlation with the total virus shed in nasal washes. A range of antibody titres against the spike protein have been demonstrated in individuals who have had severe disease requiring hospitalisation, mild to moderate disease and asymptomatic infection. It is unclear what level of antibody titres against the viral spike protein are required to prevent infection or avert disease but it is generally accepted that high-titre neutralising antibodies are required.

Both animal models in this study confirmed the safety of vaccination with ChAdOx1 nCoV-19 when the respiratory tract is exposed to large quantities ($5x10^6$ pfu) of SARS-CoV-2 virus, and demonstrated reduced lung pathology as well as reduced nasal virus shedding in ferrets which correlated negatively with the neutralizing antibody titre induced by vaccination. Here, rhesus macaques were challenged by simultaneous virus instillation to both the upper and lower respiratory tract, as in some, but not all other vaccination and challenge studies (*5-8*). Ferrets were challenged by the intranasal route only, but with the animal held vertically allowing some of the inoculum to enter the lungs. Both methods therefore result in immediate exposure of the lungs to SARS-CoV-2, whereas unless exposed to an extremely high

concentration of virus the majority of human infections are likely to infect the upper respiratory tract initially, moving to the lungs if the infection is not rapidly controlled.

Currently there are no defined correlates of protection against COVID-19 infection in humans, and the immunological thresholds required for vaccine efficacy remain undefined (*10*). In a rhesus macaque SARS-CoV-2 infection model, protection against re-challenge was associated with immunologically-mediated control of infection with both neutralising and non-neutralising antibody as well as cellular responses increasing after secondary viral exposure (*13*). It is therefore speculated that high titre neutralising antibodies with a robust cytotoxic $CD8^+$ T cell response and Th1 biased $CD4^+$ effector response will be optimal for protective immunity following SARS-CoV-2 exposure, as demonstrated here. Viral vectored vaccines have been demonstrated to induce strong immune responses in older adults and immunocompromised individuals and have been used in repeat vaccinations, subsequently inducing strong cellular and humoral immunity (*24-27*). ChAdOx1 nCoV-19 vaccination has previously been demonstrated to prevent SARS-CoV-2 mediated pneumonia in rhesus macaques (*6*), and this work is further supported and extended by the studies presented here.

# Methods

**Animals** Twelve rhesus macaques of Indian origin (Macaca mulatta) were used in this study. Study groups comprised three males and three females and all were adults aged 4 years and weighing between 4.30 and 8.24kg at time of challenge. Before the start of the experiment, socially compatible animals were randomly assigned to challenge groups, to minimise bias.

Animals were housed in compatible social groups, in cages in accordance with the UK Home Office Code of Practice for the Housing and Care of Animals Bred, Supplied or Used for Scientific Procedures (2014) and National Committee for Refinement, Reduction and Replacement (NC3Rs) Guidelines on Primate Accommodation, Care and Use, August 2006. Prior to challenge, the animals were housed at Advisory Committee on Dangerous Pathogens (ACDP) level two in cages approximately 2.5M high by 4M long by 2M deep, constructed with high level observation balconies and with a floor of deep litter to allow foraging. Following challenge, animals were transferred to ACDP Level three and housed in banks of cages of similar construction placed in directional airflow containment systems that allowed group housing and environmental control whilst providing a continuous, standardised inward flow of fully conditioned fresh air identical for all groups. Additional environmental enrichment was afforded by the provision of toys, swings, feeding puzzles and DVDs for visual stimulation. In addition to ad libitum access to water and standard old-world primate pellets, diet was supplemented with a selection of fresh vegetables and fruit. All experimental work was conducted under the authority of a UK Home Office approved project license that had been subject to local ethical review at PHE Porton Down by the Animal Welfare and Ethical Review Body (AWERB) and approved as required by the Home Office Animals (Scientific Procedures) Act 1986. Animals were sedated by intramuscular (IM) injection with ketamine hydrochloride (Ketaset, 100mg/ml, Fort Dodge Animal Health Ltd, Southampton, UK; 10mg/kg) for procedures requiring removal from their housing. None of the animals had been used previously for

experimental procedures. Twenty-eight healthy, female ferrets (Mustela putorius furo) aged 5-7 months were obtained from a UK Home Office accredited supplier (Highgate Farm, UK). The mean weight at the time of challenge was 973 g/ferret (range 825 to 1129g). Animals were housed as described previously (bioRxiv 2020.05.29.123810; doi: https://doi.org/10.1101/2020.05.29.123810). All experimental work was conducted under the authority of a UK Home Office approved project licence that had been subject to local ethical review at PHE Porton Down by the Animal Welfare and Ethical Review Body (AWERB). One animal in the ChAdOx1 nCoV-19 prime only group steadily lost weight from arrival at the facility (5 days prior to vaccination) and throughout the post-vaccination follow-up and was sacrificed on welfare grounds at day 14 of the study. As the weight loss was observed from arrival it was not deemed vaccine related, therefore all immunological data from this animal has been excluded from the analysis.

**Vaccinations** Rhesus macaques received $2.5x10^{10}$vp ChAdOx1 nCoV-19 administered in 100ml intramuscularly or received 100ml of phosphate buffered saline intramuscularly and were challenged with SARS-CoV-2 twenty-seven days later. Ferrets were randomly assigned to ChAdOx1 nCoV-19 and ChAdOx1 GFP vaccinated groups. An identifier chip (Bio-Thermo Identichip, Animalcare Ltd, UK) was inserted subcutaneously into the dorsal cervical region of each animal. Ferrets were immunised with $2.5 \times 10^{10}$ virus particles of ChAdOx1 nCoV-19 or ChAdOx1 GFP intramuscularly administered as a 100ml volume into the hind leg. Twenty-eight days after vaccination, half of the vaccinated animals were challenged with SARS-CoV-2, while the other half received a booster dose of ChAdOx1 nCoV-19 of ChAdOx1 GFP and were challenged with SARS-CoV-2 a further twenty-eight days later.

**Enzyme-linked immunosorbent assay** Maxisorp plates (Nunc) were coated overnight at 4°C with 250 ng/well spike protein in PBS, prior to blocking with 100 µl of casein in PBS (Thermo Fisher) for 1hr at RT. NHP serum was serially diluted 2x in casein in PBS was incubated at RT for 1hr. Antibodies were detected using affinity-purified polyclonal antibody alkaline phosphatase-labelled goat-anti-monkey IgG (Rocklands Laboratories), anti-monkey IgM (Rockland Laboratories) or anti-monkey IgA (Rockland Laboratories) in casein and developed with NPP-substrate (Sigma) and read at 405 nm. All wells were washed at least 3x with PBST 0.05% tween in between steps. Endpoint titers were calculated as follows: the $\log_{10}$ OD against $\log_{10}$ sample dilution was plotted and a regression analysis of the linear part of this curve allowed calculation of the endpoint titer with an OD of three times the background. Ferret serum was diluted in casein and incubated at RT for 2hr. Antibodies were detected using affinity-purified polyclonal antibody HRP-labelled goat-anti-ferret IgG (Abcam) in casein and TMB highest sensitivity (Abcam), developed for 12 minutes, and reaction was stopped using $H_2SO_4$ and read at 450 nm. Anti-spike IgM or IgA antibodies were detected with alkaline Phosphatase conjugated anti-ferret IgM (Rockland Laboratories) or anti-ferret IgA (Sigma), development with NPP-substrate and read at 405 nm. All wells were washed at least 3x with PBST 0.05% tween in between steps. Ferret samples were run against a standard positive pool of serum generated from ChAdOx1 nCoV-19 vaccinated ferrets with high endpoint titre. Due to high levels of non-specific responses, background was defined as the mean + 2x stdev of all animals at day 0.

**Plaque Reduction Neutralisation Assay** Heat-inactivated (56°C for 30 min) serum samples were serially diluted and incubated with approximately 60 PFU of wild type SARS-CoV-2 (2019-nCoV/Victoria/1/2020), for 1 h at 37°C in 5% $CO_2$. Samples were then incubated with Vero E6 [Vero 76, clone E6 (ECACC 85020206), European Collection of Authenticated Cell Cultures, UK] monolayers in 24-well plates (Nunc, ThermoFisher Scientific, Loughborough, UK) under MEM (Life Technologies, California, USA) containing 1.5% carboxymethylcellulose (Sigma), 5% (v/v) foetal calf serum (Life Technologies) and 25mM HEPES buffer (Sigma). After incubation, at 37°C for 96 hours, plates were fixed overnight with 20% (w/v) formalin/PBS, washed with tap water and stained with methyl crystal violet solution (0.2% v/v) (Sigma). The neutralising antibody titres were defined as the serum dilutions resulting in a 50% reduction relative to the total number of plaques counted without antibody by using Probit analysis written in R programming language for statistical computing and graphics. An internal positive control for the PRNT assay was run using a sample of human MERS convalescent serum known to neutralise SARS-CoV-2 (National Institute for Biological Standards and Control, UK)

**Micro neutralisation test (mVNT) using lentiviral-based pseudotypes bearing the SARS-CoV-2 Spike.** Lentiviral-based SARS-CoV-2 pseudotyped viruses were generated in HEK293T cells incubated at 37 °C, 5% $CO_2$ as previously described (npj Vaccines (2020) 5:69; https://doi.org/10.1038/s41541-020-00221-3). Briefly, cells were seeded at a density of 7.5 $x\,10^5$ in 6 well dishes, before being transfected with plasmids as follows: 500 ng of SARS-CoV-2 spike, 600 ng p8.91 (encoding for HIV-1 gag-pol), 600 ng CSFLW (lentivirus backbone expressing a firefly luciferase reporter gene), in Opti-MEM (Gibco) along with 10 µL PEI (1 µg/mL) transfection reagent. A 'no glycoprotein' control was also set up using the pcDNA3.1 vector instead of the SARS-CoV-2 S expressing plasmid. The following day, the transfection mix was replaced with 3 mL DMEM with 10% FBS (DMEM-10%) and incubated for 48 and 72 hours, after which supernatants containing pseudotyped SARS-CoV-2 (SARS-CoV-2 pps) were harvested, pooled and centrifuged at 1,300 x *g* for 10 minutes at 4 °C to remove cellular debris. Target HEK293T cells, previously transfected with 500 ng of a human ACE2 expression plasmid (Addgene, Cambridge, MA, USA) were seeded at a density of $2 \times 10^4$ in 100 µL DMEM-10% in a white flat-bottomed 96-well plate one day prior to harvesting SARS-CoV-2 pps. The following day, SARS-CoV-2 pps were titrated 10-fold on target cells, and the remainder stored at -80 °C. For mVNTs, NHP plasma was diluted 1:10 and ferret plasma diluted 1:20 in serum-free media and 50 µL was added to a 96-well plate in triplicate and titrated 2-fold. A fixed titred volume of SARS-CoV-2 pps was added at a dilution equivalent to $10^5$ signal luciferase units in 50 µL DMEM-10% and incubated with sera for 1 hour at 37 °C, 5% $CO_2$ (giving a final sera dilution of 1:40). Target cells expressing human ACE2 were then added at a density of 2 $x\,10^4$ in 100 µL and incubated at 37 °C, 5% $CO_2$ for 72 hours. Firefly luciferase activity was then measured with BrightGlo luciferase reagent and a Glomax-Multi$^+$ Detection System (Promega, Southampton, UK). Pseudotyped virus neutralisation titres were expressed as a 50% neutralisation dose ($ND_{50}$) using a Spearman and Karber formula.

**ELISpot** PBMCs from rhesus macaques and ferrets were isolated from whole blood by layering over Lymphoprep (density 1.077g) and centrifugation for 30 minutes at 1000g. PBMCs were collected

from the interface, washed with Hanks Balanced Salt Solution (HBSS) prior to resuspension in complete media (RPMI supplemented with 10% FCS, Pent-Strep, L-Glut and Hepes). IFNg ELISpot assay was performed using NHP IFNg (Mabtech) or Ferret IFNg ELISpot$^{BASIC}$ Kit according to the manufacturer's protocol (MABtech). PBMCs were plated at a concentration of 250 000 cells per well (NHPs) or 100 000 cells per well (Ferrets) and were stimulated overnight (18 to 20 hours) with four contiguous peptide pools spanning the length of the SARS-CoV-2 spike protein sequence at a concentration of 2µg/mL per peptide (Mimotopes) (Table S7). Spots were counted and analysed on an AID ELISpot Reader (AID). Spot forming units (SFU) per $1.0x10^6$ PBMCs were summed across the 4 peptide pools for each animal after subtraction of background response (media and PBMC only wells). Simultaneous production of IFNg, IL13 and IL5 was detected with a custom FLUROspot$^{FLEX}$ kit (Mabtech) using anti-monkey IFNg FluroSpot set 490, anti-monkey IL13 FluroSpot set 550 and anti-human IL5 FluroSpot set 640. ELISpot was performed with the same stimulation conditions as above (200 000 cells and 4 peptide pools), with plates developed according to the manufacturer's instructions. Spot were enumerated using Mabtech IRIS$^{TM}$ reader and analysed with SpotReader software (Mabtech). Post-challenge NHP ELISpot were performed on PBMCs isolated over a Ficoll-Paque Plus (GE Healthcare, USA) density gradient and anti-human/simian IFNg kit (Mabtech). 200 000 cells per well were stimulated with 3 pools of SARS-CoV-2 peptides (Table S7, Pool 1 peptides 1 to 96, Pool 2 peptides 97 to 192, Pool 3 peptides 193 to 316) at a final concentration of 1.7µg/ml, Phorbol 12-myristate (Sigma-Aldrich Dorset, UK) (100 ng/ml) and ionomycin (CN Biosciences, Nottingham, UK) (1 mg/ml) were used as a positive control. ELISpot plates were analysed using the CTL scanner and software (CTL, Germany) and further analysis carried out using GraphPad Prism (version 8.0.1) (GraphPad Software, USA).

**Measurement of NHP serum cytokines** Rhesus macaque PBMCs were stimulated for 16 hours with 2 pools of SARS-CoV-2 peptides (S1 and S2) and cytokine measured using MescoScaleDiscovery (MSD) Technology V-PLEX Proinflammaotry Panel 1 NHP kit according to the manufacturer's instructions. $Log_{10}$ Fold Change ($Log_{10}FC$) was calculated by dividing concentration detected in stimulated wells by unstimulated wells, baseline detectable level of each cytokine was set at 0.01mg.

**Intracellular cytokine staining** Ferret PBMCs were stimulated for 18-20 hours with 2 pools of SARS-CoV-2 spike peptides (S1-pool 1 and pool 2 or S2-pool 3 and pool 4) at a final concentration of 2µg/ml or ConA in the presence of golgi-stop (BD) and golgi-plug (BD). Cells were surface stained with anti-mouse/rat/human CD3 Alexa 405 (Clone PC3/188A) (Santa Cruz Biotechnology), anti-human CD8 APCCy7 (Clone OKT8) (Thermofisher) and live-dead aqua (Thermofisher), fixed with Fix-Perm solution prior to intracellular staining with anti-bovine IFNg PE (Clone CC302) (Abserotec) and anti-mouse TNFa A647 (Clone MP6-XT22) (D28 samples). Data was acquired on a BD Fortessa and analysed in FlowJo version 9 or above. Data is presented total spike response, by summing together the frequency of cytokine positive cells detected in S1 and S2 stimulated wells after background subtraction of media stimulated cells.

**Challenge** Animals were challenged with SARS-CoV-2 (VERO/hSLAM cell passage 3 (Victoria/1/2020)) at a final challenge dose of $5x10^6$ pfu. NHPs received 2ml intratracheally followed by 1ml intranasally, ferrets received a total of 1ml split equally between both nares.

Prior to challenge ferrets were sedated by intramuscular injection of ketamine/xylazine (17.9 mg/kg and 3.6 mg/kg bodyweight). Challenge virus prepared as described previously (*bioRxiv* **2**, 2020.05.29.123810 (2020) and **doi:** https://doi.org/10.1101/2020.09.17.301093) was delivered by intranasal instillation (1.0 mL total, 0.5 mL per nostril) diluted in phosphate buffered saline (PBS). Nasal washes were obtained by flushing ferret nasal cavities with 2 mL PBS. Throat swabs were collected using a standard swab (Sigma Virocult®) gently stroked across the back of the pharynx in the tonsillar area. Throat swabs were processed, and aliquots stored in viral transport media (VTM) and AVL at ≤-60°C until assay. Clinical signs of disease were monitored as described previously *bioRxiv* **2**, 2020.05.29.123810 (2020). The necropsy procedures were also as described previously *bioRxiv* **2**, 2020.05.29.123810 (2020).

**Computed Tomography (CT) Radiology of NHPs** CT scans were collected from sedated macaques using a 16 slice Lightspeed CT scanner (General Electric Healthcare, Milwaukee, WI, USA) in the prone and supine position. The change in position assists differentiation between pulmonary changes due to gravity dependant atelectasis from ground glass opacity at the lung bases caused by COVID. All axial scans were performed at 120KVp, with Auto mA (ranging between 10 and 120) and were acquired using a small scan field of view. Rotation speed was 0.8s. Images were displayed as an 11cm field of view. To facilitate full examination of the cardiac / pulmonary vasculature, lymph nodes and extrapulmonary tissues, Niopam 300 (Bracco, Milan, Italy), a non-ionic, iodinated contrast medium, was administered intravenously (IV) at 2ml/kg body weight and scans collected immediately after injection and ninety seconds from the mid-point of injection. Scans were evaluated by an expert thoracic radiologist, blinded to the animal's treatment and clinical status for the presence of COVID disease features: ground glass opacity (GGO), consolidation, crazy paving, nodules, peri-lobular consolidation; distribution - upper, middle, lower, central 2/3, peripheral, bronchocentric) and for pulmonary embolus.

The extent of lung involvement was estimated (<25%, 25-50%, 51-75%, 76-100%) and quantified using a scoring system developed for COVID disease, as follows:

*COVID disease pattern*: Nodule(s): Score 1 for 1, 2 for 2 or 3, 3 for 4 or more. GGO: Score 1 if measures < 1 cm, 2 if 1 to 2 cm, 3 if 2 -3 cm, 4 if > 3 cm. Consolidation Score: 2 if measures < 1 cm, 4 if 1 to 2 cm, 6 if 2 -3 cm, 8 if > 3 cm. *Zone classification:* Each side of the lung was divided (from top to bottom) into three zones: The upper zone (above the carina), the middle zone (from the carina to the inferior pulmonary vein), and the lower zone (below the inferior pulmonary vein). Each zone was then divided into two areas: the anterior area (the area before the vertical line of the midpoint of the diaphragm in the sagittal position) and the posterior area (the area after the vertical line of the mid-point of the diaphragm in the sagittal position). This results in 12 zones in total. *Measures:* COVID pattern score = Nodule score + GGO score + consolidation score. Distribution (Zone) score = number of zones with disease, maximum score 12. Total CT score = COVID pattern score + Distribution (zone) score

**Whole Blood Immunophenotyping** Assays were performed using 50µl of heparinised blood incubated for 30 minutes at room temperature with optimal dilutions of the following antibodies: anti-CD3-AF700, anti-CD4-APC-H7, anti-CD8-PerCP-Cy5.5, anti-CD95-Pe-Cy7, anti-CD14-PE, anti-HLA-DR-BUV395, anti-CD25-FITC (all from BD Biosciences, Oxford, UK); anti-γδ-TCR-BV421, anti-CD16-BV786, anti-CD20-PE-Dazzle (all from BioLegend); and amine reactive fixable viability stain red (Life Technologies); all prepared in brilliant stain buffer (BD Biosciences). Red blood cell contamination was removed using a Utilyse reagent kit as per the manufacturer's instructions (Agilent). BD Compbeads (BD Biosciences) were labelled with the above fluorochromes for use as compensation controls. Following antibody labelling, cells and beads were fixed in a final concentration of 4% paraformaldehyde solution (Sigma Aldrich, Gillingham, UK) prior to flow cytometric acquisition. Cells were analysed using a five laser LSRII Fortessa instrument (BD Biosciences) and data were analysed using FlowJo (version 9.7.6, BD Biosciences). Immediately prior to flow cytometric acquisition, 50 µl of Truecount bead solution (Beckman Coulter) was added to each sample. Leukocyte populations were identified using a forward scatter-height (FSC-H) versus side scatter-area (SSC-A) dot plot to identify the lymphocyte, monocyte and granulocyte populations, to which appropriate gating strategies were applied to exclude doublet events and non-viable cells. Lymphocyte sub populations including T-cells, NK-cells, NKT-cells and B-cells were delineated by the expression pattern of CD3, CD20, CD95, CD4, CD8, CD127, CD25, CD16 and the activation and inhibitory markers HLA-DR and PD-1. Classical- and non-classical-monocytes were identified by expression pattern of HLA-DR, CD14 and CD16. Granulocyte populations were delineated into neutrophils and eosinophils by expression of HLA-DR and CD14.

**Total Viral RNA detection by Polymerase Chain Reaction** RNA was isolated from nasal wash, throat swabs and BAL. Samples were inactivated in AVL (Qiagen) and ethanol. Downstream extraction was then performed using the BioSprint™96 One-For-All vet kit (Indical) and Kingfisher Flex platform as per manufacturer's instructions. Reverse transcription-quantitative polymerase chain reaction (RT-qPCR) targeting a region of the SARS-CoV-2 nucleocapsid (N) gene was used to determine viral loads and was performed using TaqPath™ 1-Step RT-qPCR Master Mix, CG (Applied Biosystems™), 2019-nCoV CDC RUO Kit (Integrated DNA Technologies) and QuantStudio™ 7 Flex Real-Time PCR System. Sequences of the N1 primers and probe were: 2019-nCoV_N1-forward, 5' GACCCCAAAATCAGCGAAAT 3'; 2019-nCoV_N1-reverse, 5' TCTGGTTACTGCCAGTTGAATCTG 3'; 2019-nCoV_N1-probe, 5' FAM-ACCCCGCATTACGTTTGGTGGACC-BHQ1 3'. The cycling conditions were: 25°C for 2 minutes, 50°C for 15 minutes, 95°C for 2 minutes, followed by 45 cycles of 95°C for 3 seconds, 55°C for 30 seconds. The quantification standard was in vitro transcribed RNA of the SARS-CoV-2 N ORF (accession number NC_045512.2) with quantification between $1 \times 10^1$ and $1 \times 10^6$ copies/µl. Positive samples detected below the limit of quantification (LOQ) were assigned the value of 5 copies/µl, whilst undetected samples were assigned the value of < 2.3 copies/µl, equivalent to the assay's lower limit of detection (LLOD).

**Histopathology NHPs:** Each animal was assigned a histology number for blinding purposes. The following samples from each animal was fixed in 10% neutral-buffered formalin, processed to paraffin wax and 4 µm thick sections cut and stained with haematoxylin and eosin (H&E); respiratory tract (left

cranial and caudal lung lobes), trachea, larynx, tonsil, liver, kidney, spleen, mediastinal lymph node, and small and large intestine. Tissue sections were examined by light microscopy and evaluated subjectively and semi-quantitatively using a scoring system. Pathologists were blinded to treatment and group details and the slides randomised prior to examination in order to prevent bias (blind evaluation). The slides were reviewed independently by three board-certified veterinary pathologists. For the lung, three sections from each left lung lobe were sampled from different locations: proximal, medial and distal to the primary lobar bronchus. The scoring system was applied using the following parameters and scores: *Parameters:* Bronchial epithelial degeneration/necrosis with presence of exudates and/or inflammatory cell infiltration. Bronchiolar (primarily terminal) epithelial degeneration/necrosis with presence of exudates and/or inflammatory cell infiltration. Perivascular inflammatory infiltrates (cuffing). Peribronchiolar inflammatory infiltrates (cuffing). Acute diffuse alveolar damage (necrosis of pneumocytes). Alveolar cellular exudate and oedema and/or fibrin. Alveolar septal inflammatory cells and cellularity. *Scores:* 0 = Normal 1 = Minimal 2 = Mild 3 = Moderate 4 = Severe. **Ferrets**: A semiquantitative scoring system was developed to compare the severity of the lung lesions for each individual animal and among groups. This scoring system was applied independently to the cranial and caudal lung lobe tissue sections using the following parameters and scores: *Parameters:* Bronchial inflammation with presence of exudates and/or inflammatory cell infiltration. Bronchiolar inflammation with presence of exudates and/or inflammatory cell infiltration. Perivascular inflammatory infiltrates (cuffing). Infiltration of alveolar walls and spaces by inflammatory cells, mainly mononuclear *Scores:* 0 = None 1 = Minimal 2 = Mild 3 = Moderate 4 = Severe

**Detection of virus by RNAscope** An in-situ hybridisation method used on formalin-fixed, paraffin-embedded tissues was used to identify the SARS-CoV-2 virus in both lung lobes of NHPs. Briefly, tissues were pre-treated with hydrogen peroxide for 10 mins (RT), target retrieval for 15 mins (98-101□C) and protease plus for 30 mins (40□C) (all Advanced Cell Diagnostics). A V-nCoV2019-S probe (Advanced Cell Diagnostics) targeting the S-protein gene was incubated on the tissues for 2 hours at 40□C. Amplification of the signal was carried out following the RNAscope protocol (RNAscope 2.5 HD Detection Reagent – Red) using the RNAscope 2.5 HD red kit (Advanced Cell Diagnostics). Digital image analysis (Nikon NIS-Ar software) was carried out in order to calculate the total area of the lung section positive for viral RNA.

# Declarations

**Acknowledgments:** The authors would like to thank D. Pulido and T. Tipton for provision of reagents, D. Gkolfinos, A. Mabbutt, K. Gooch, J. Gouriet, K. Godwin, J. Logue, J. Patterson for assistance with sample processing. The authors would also like to thank P. Yeates, M. Dennis, I. Taylor and all Biological Investigations Group staff for animal husbandry and management and assistance with in vivo procedures, N. Coombes, E. Penn, K. Buttigieg, R. Watson, N. McLeod, C. Turner, T. Hender and S. Findlay-Wilson for assistance with experimental work and M. Elmore, E. Rayner and G. Pearson for data analysis or review.

**Funding:** This report is independent research funded by the National Institute for Health Research (UKRI Grant Ref: MC_PC_19055, NIHR Ref: COV19 OxfordVacc-01). The views expressed in this publication are those of the author(s) and not necessarily those of the National Institute for Health Research or the Department of Health and Social Care.

**Author Contributions:** A.J.S, S.T., A.D.W, H.E.H, D.W., S.B-R, N.T., C.C., L.A, M.A, K.B., E.B., L.H., C.K., S.L., C.S., L.S., N.W., S.S, F.J.S performed experiments. A.J.S., S.T, A.W., L.A., P.B., B.C., R.C., S.F., C.G, D.H., L.H., V.L., D.N., K.R., H.S., M.U., N.W., performed animal procedures and/or sample processing. T.L., A.J.S., K.M.T, S.T, A.D.W, H.E.H, D.W., S.B.J., N.T., C.S., L.S., G.S., F.V.G., D.B., S.S, F.J.S, analyzed data. T.L., S.C., M.C., S.C.G. designed the study. T.L., A.J.S., S.C.G. wrote the manuscript.

**Competing interests:** SCG is co-founder and board member of Vaccitech (collaborators in the early development of this vaccine candidate) and named as an inventor on a patent covering use of ChAdOx1-vectored vaccines and a patent application covering this SARS-CoV-2 vaccine. TL is named as an inventor on a patent application covering this SARS-CoV-2 vaccine and consultant to Vaccitech;

**Data and Materials availability:** All data is available in the main text or the supplementary materials.

# References

1. F. P. Polack *et al.*, Safety and Efficacy of the BNT162b2 mRNA Covid-19 Vaccine. *N Engl J Med*, (2020).
2. M. Voysey *et al.*, Safety and efficacy of the ChAdOx1 nCoV-19 vaccine (AZD1222) against SARS-CoV-2: an interim analysis of four randomised controlled trials in Brazil, South Africa, and the UK. *Lancet*, (2020).
3. Q. Gao *et al.*, Development of an inactivated vaccine candidate for SARS-CoV-2. *Science* **369**, 77-81 (2020).
4. H. Wang *et al.*, Development of an Inactivated Vaccine Candidate, BBIBP-CorV, with Potent Protection against SARS-CoV-2. *Cell* **182**, 713-721 e719 (2020).
5. N. B. Mercado *et al.*, Single-shot Ad26 vaccine protects against SARS-CoV-2 in rhesus macaques. *Nature*, (2020).
6. N. van Doremalen *et al.*, ChAdOx1 nCoV-19 vaccine prevents SARS-CoV-2 pneumonia in rhesus macaques. *Nature*, (2020).
7. K. S. Corbett *et al.*, Evaluation of the mRNA-1273 Vaccine against SARS-CoV-2 in Nonhuman Primates. *N Engl J Med*, (2020).
8. J. Yu *et al.*, DNA vaccine protection against SARS-CoV-2 in rhesus macaques. *Science*, (2020).
9. A. Patel, et al., Intradermal-delivered DNA vaccine provides anamnestic protection in a rhesus macaque SARS-CoV-2 challenge model. *bioRxiv*, (2020).
10. A. Chandrashekar *et al.*, SARS-CoV-2 infection protects against rechallenge in rhesus macaques. *Science*, (2020).

11. W. Deng *et al.*, Primary exposure to SARS-CoV-2 protects against reinfection in rhesus macaques. *Science* **369**, 818-823 (2020).
12. K. Bewley et al., Immunological and pathological outcomes of SARS-CoV-2 challenge after formalin-inactivated vaccine immunisation of ferrets and rhesus macaques. *BioRXiv*, (2020).
13. P. M. Folegatti *et al.*, Safety and immunogenicity of the ChAdOx1 nCoV-19 vaccine against SARS-CoV-2: a preliminary report of a phase 1/2, single-blind, randomised controlled trial. *Lancet*, (2020).
14. F. J. Salguero, White, A. D., Slack, G. S. Fotheringham, S. A., Comparison of Rhesus and Cynomolgus macaques as an authentic model for COVID-19. *bioRxiv*, (2020).
15. M. R. Chetan *et al.*, Chest CT screening for COVID-19 in elective and emergency surgical patients: experience from a UK tertiary centre. *Clin Radiol* **75**, 599-605 (2020).
16. N. C. Pedersen, An update on feline infectious peritonitis: virology and immunopathogenesis. *Vet J* **201**, 123-132 (2014).
17. A. M. Arvin *et al.*, A perspective on potential antibody-dependent enhancement of SARS-CoV-2. *Nature* **584**, 353-363 (2020).
18. C. T. Tseng *et al.*, Immunization with SARS coronavirus vaccines leads to pulmonary immunopathology on challenge with the SARS virus. *PLoS One* **7**, e35421 (2012).
19. P. L. Collins, B. S. Graham, Viral and host factors in human respiratory syncytial virus pathogenesis. *J Virol* **82**, 2040-2055 (2008).
20. M. Connors *et al.*, Enhanced pulmonary histopathology induced by respiratory syncytial virus (RSV) challenge of formalin-inactivated RSV-immunized BALB/c mice is abrogated by depletion of interleukin-4 (IL-4) and IL-10. *J Virol* **68**, 5321-5325 (1994).
21. P. A. Jorquera, L. Anderson, R. A. Tripp, Understanding respiratory syncytial virus (RSV) vaccine development and aspects of disease pathogenesis. *Expert Rev Vaccines* **15**, 173-187 (2016).
22. H. W. Kim *et al.*, Respiratory syncytial virus disease in infants despite prior administration of antigenic inactivated vaccine. *Am J Epidemiol* **89**, 422-434 (1969).
23. F. P. Polack *et al.*, A role for immune complexes in enhanced respiratory syncytial virus disease. *J Exp Med* **196**, 859-865 (2002).
24. M. N. Ramasamy *et al.*, Safety and immunogenicity of ChAdOx1 nCoV-19 vaccine administered in a prime-boost regimen in young and old adults (COV002): a single-blind, randomised, controlled, phase 2/3 trial. *Lancet* **396**, 1979-1993 (2021).
25. L. Coughlan *et al.*, Heterologous Two-Dose Vaccination with Simian Adenovirus and Poxvirus Vectors Elicits Long-Lasting Cellular Immunity to Influenza Virus A in Healthy Adults. *EBioMedicine* **29**, 146-154 (2018).
26. L. R. Baden *et al.*, Assessment of the Safety and Immunogenicity of 2 Novel Vaccine Platforms for HIV-1 Prevention: A Randomized Trial. *Ann Intern Med* **164**, 313-322 (2016).
27. B. P. Ndiaye *et al.*, Safety, immunogenicity, and efficacy of the candidate tuberculosis vaccine MVA85A in healthy adults infected with HIV-1: a randomised, placebo-controlled, phase 2 trial.

*Lancet Respir Med* **3**, 190-200 (2015).

# Figures

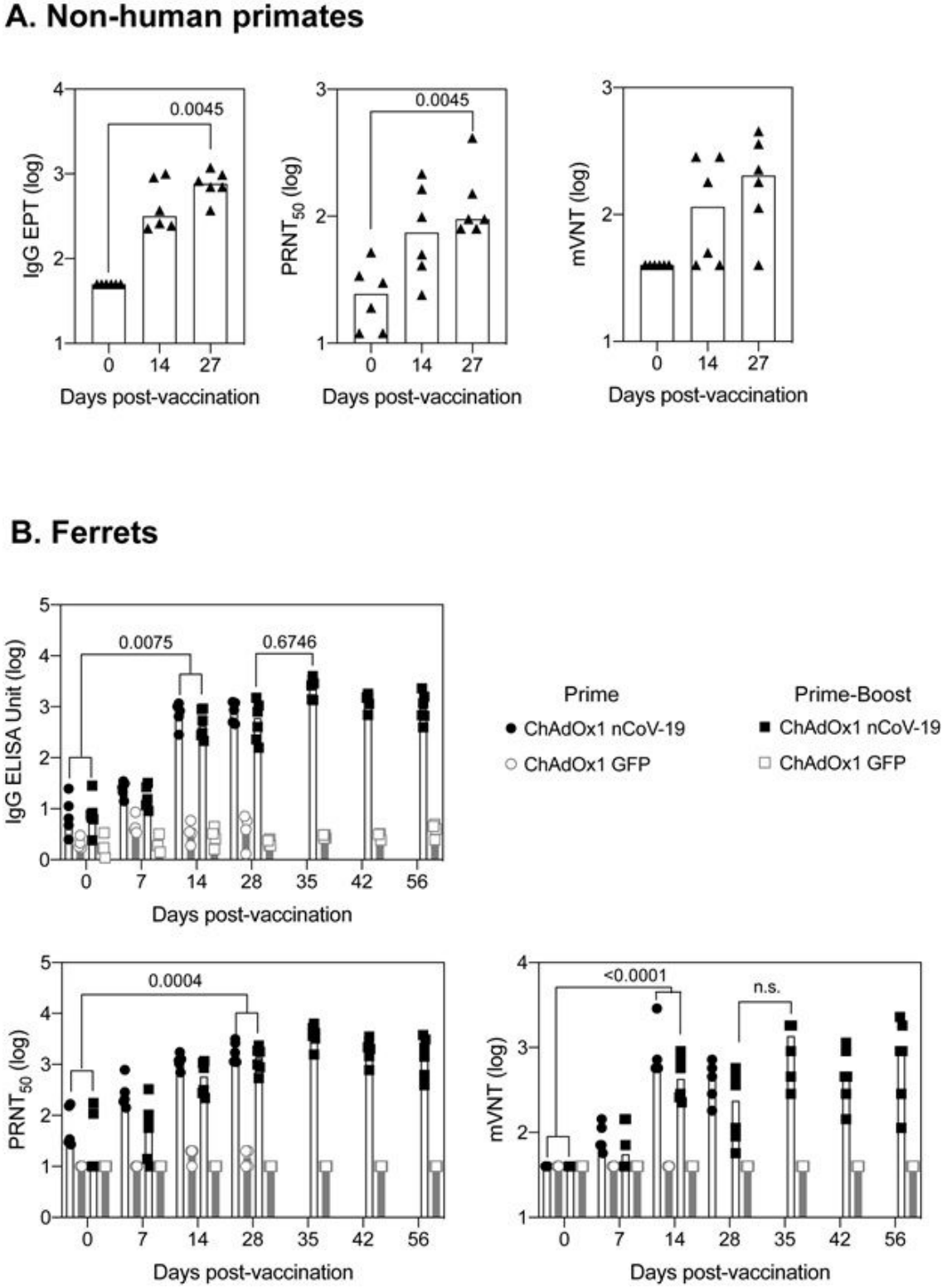


**Figure 1**

Antibody responses in rhesus macaques and ferrets following vaccination with ChAdOx1 nCoV-19. a. Anti-spike responses, ELISA and neutralisation titres (PRNT50) were measured in the serum and pseudoneutralisation titres (mVNT ID50) in the plasma of rhesus macaque on days 0, 14 and 27 post vaccination. Data was analysed with a Friedman one-way anova and post-hoc test. Responses in rhesus macaques vaccinated with PBS were below the limit of detection. b. Anti-spike responses, ELISA and neutralisation titres measured in the serum and pseudoneutralisation titres measured in the plasma of ferrets following vaccination with ChAdOx1 nCoV-19 or ChAdOx1 GFP. Data was analysed by a one-way anova and post-hoc test comparing all ChAdOx1 nCoV-19 vaccinated to all ChAdOx1 GFP at each relevant timepoint.

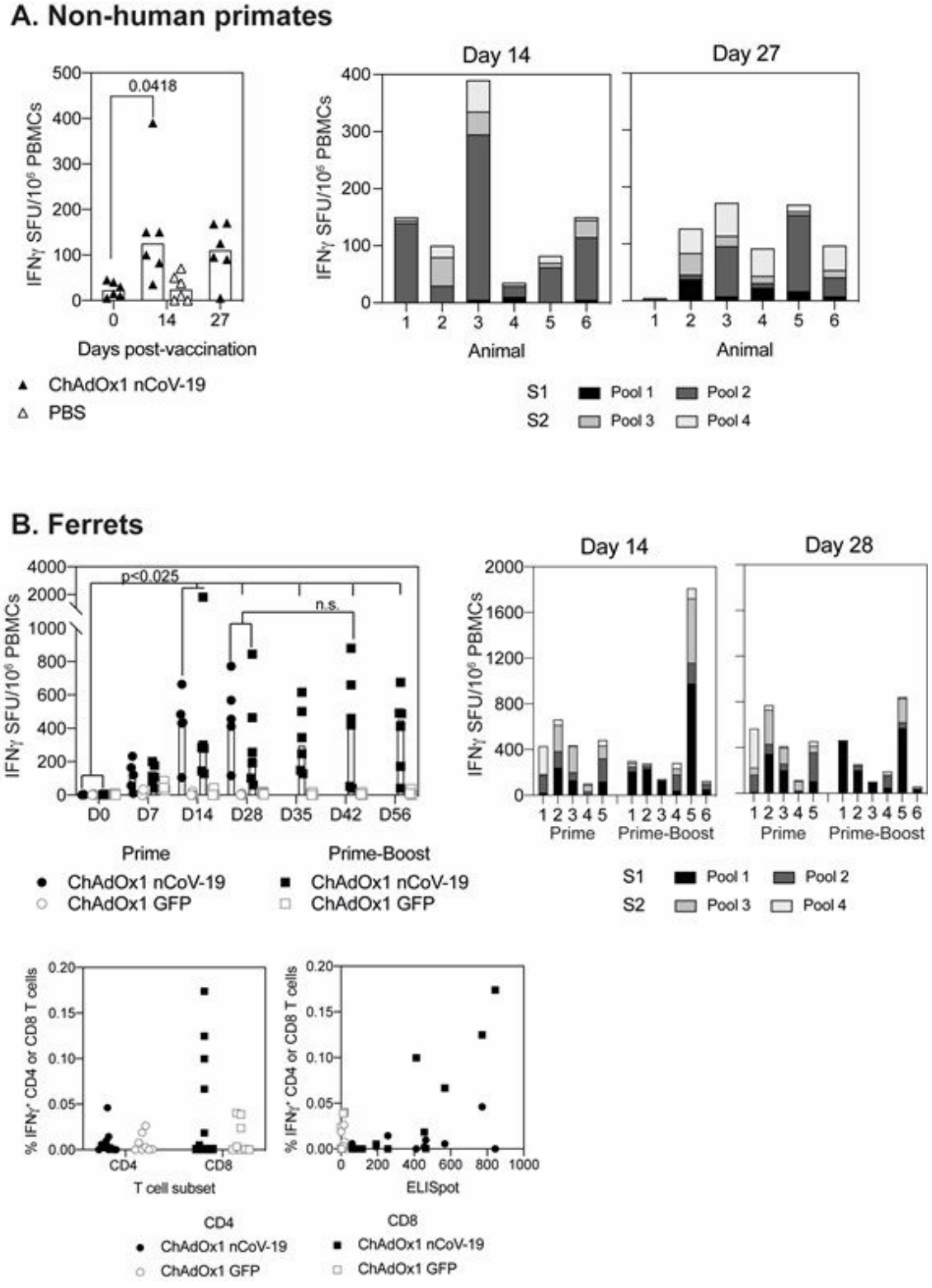


## Figure 2

Spike-specific T cell response in rhesus macaques a. and ferrets b. monitored by IFNy ELISpot following vaccination and ICS (ferrets only). Response from ChAdOx1 nCoV-19 vaccinated NHPs was analysed with a Friedman one-way anova and post-hoc test. Response in ferrets was analysed with a non-parametric one-way anova (Kruskal Wallis) and post-hoc Dunn's multiple comparison test. A significant increase in the response compared to Day 0 was observed from day 14 onwards, with no statistically

significant increase in the T cell response following booster vaccination. T cell responses in ferrets were measured by intracellular cytokine staining on day 28 post-vaccination and compared to responses measured by IFNy ELISpot.

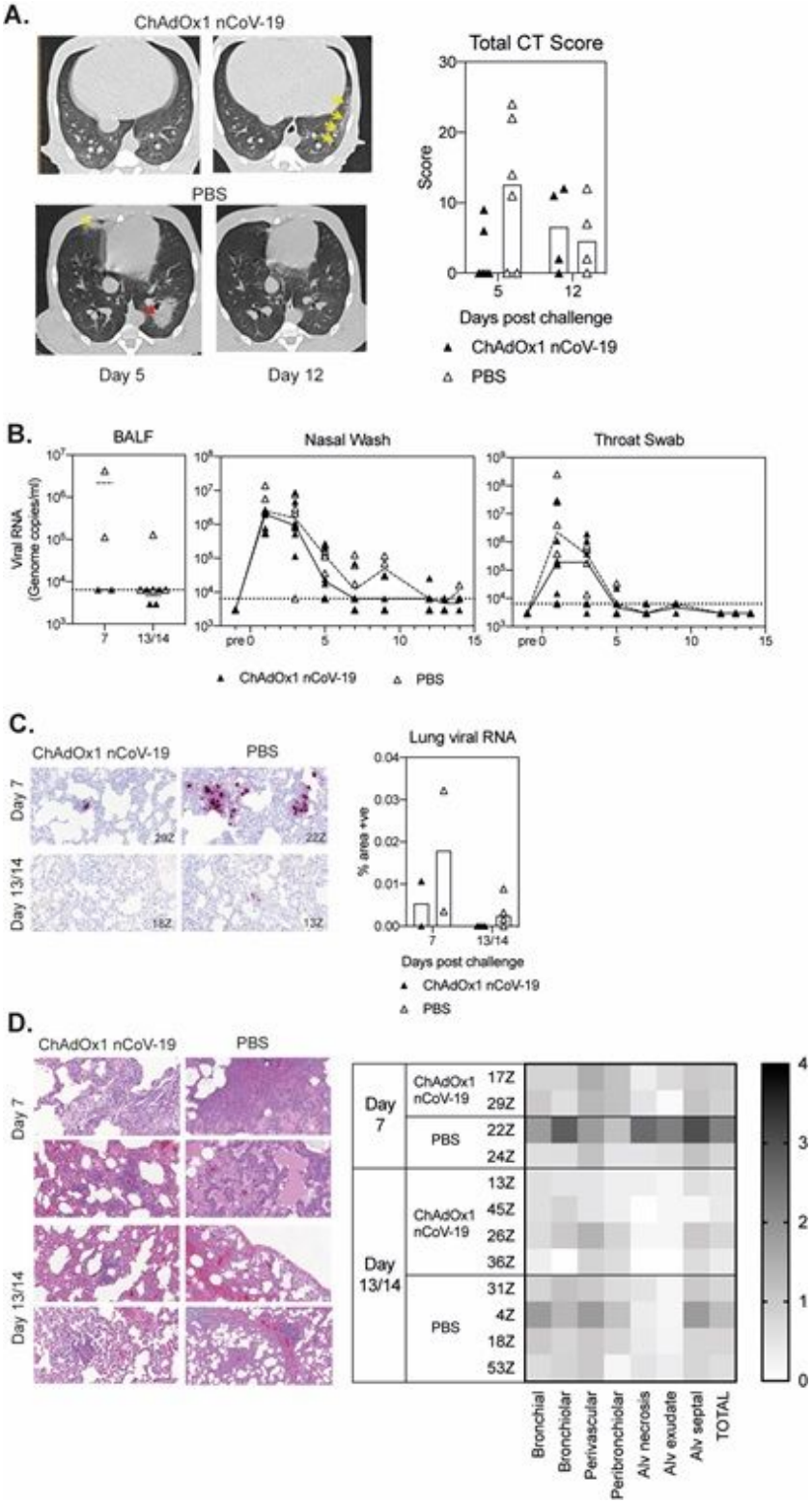


## Figure 3

Challenge of rhesus macaques with SARS-CoV-2. a. Representative CT scans of a vaccinated male (top panel), normal appearance at D5, unilateral mild abnormalities at D12, with peripheral ground glass

opacity (GGO) marked by yellow arrows, and PBS vaccinated female (lower panel) with bilateral disease on D5, mid-lobe GGO (yellow arrow), left lower lobe consolidated organizing pneumonia pattern (red arrow), resolved by D12. Graph represents the total CT score representing disease severity. b. Viral RNA quantitation in bronchoalveolar lavage fluid (BALF), nasal washes and throat swabs. c. RNA staining at Day 7 (top) and day 13/14 (bottom) after challenge, graph represents the quantification of viral RNA by ISH in the lung from all animals at 7 and 13/14 days after challenge. d. Histopathology at Day 7 (top 2 panels), day 13/14 (bottom 2 panels) after challenge and heatmap showing relative frequency of histopathological abnormalities detected in different lung locations.

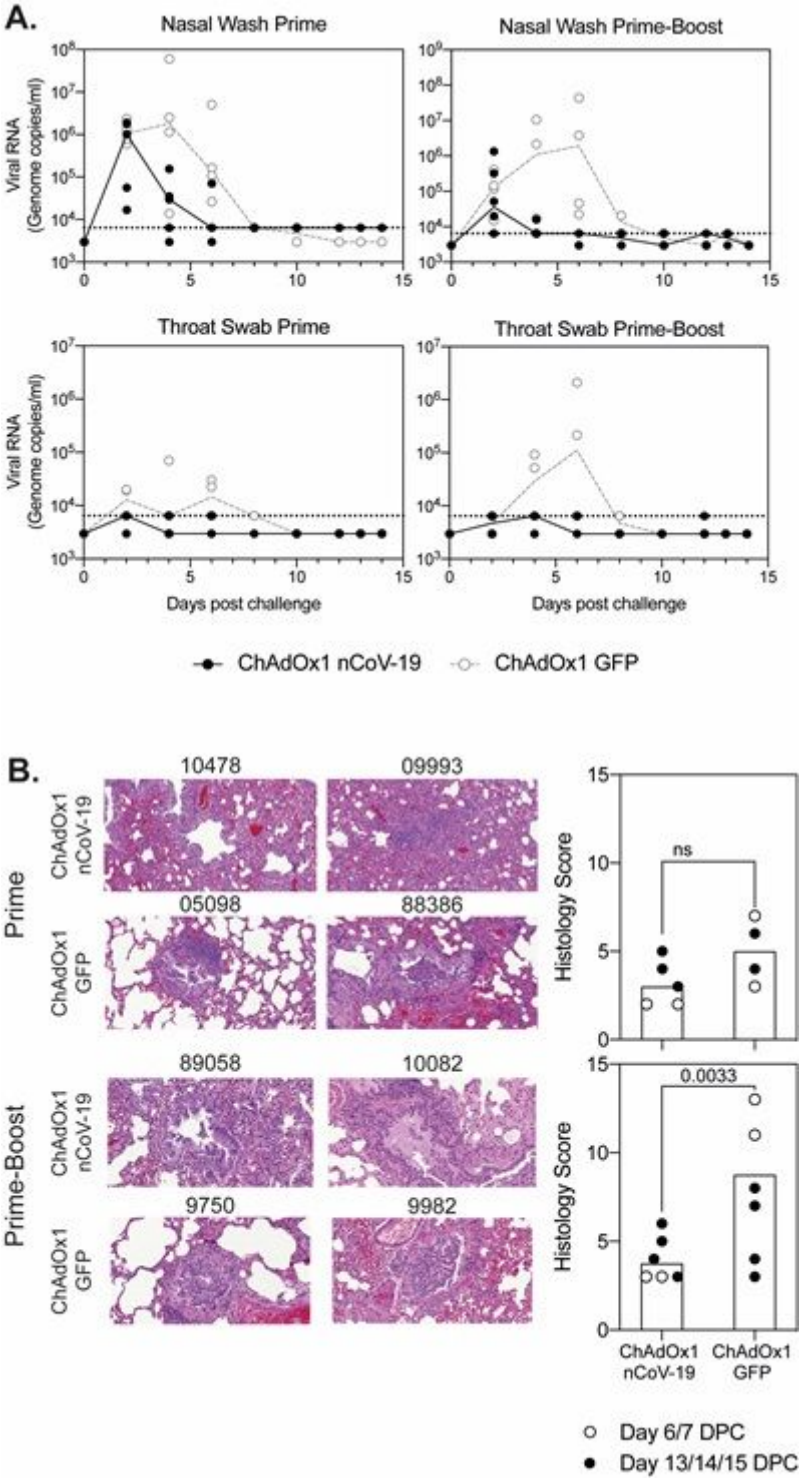

## Figure 4

Challenge of ferrets with SARS-CoV-2 a. Quantification of virus RNA by PCR in nasal washes and throat swabs in ferrets vaccinated with ChAdOx1 nCoV-19 (black closed) or ChAdOx1 GFP controls (grey open) following challenge with SARS-CoV-2. Limit of quantification in the assay is indicated as dotted line on the graph. b. Histopathology was performed on lung sections of animals culled 1 week after challenge (day 6 or 7) (presented) or 2 weeks after challenge (days 13, 14 or 15) (Fig. S5). Graphs represent the total histopathological score of each animal. Data points represent each animal, with bars denoting the median per group. Histopathological score data was analysed with a 2-way anova to determine the effect of vaccination and day of cull; no difference between days was observed, significant differences between groups is denoted on the graph.

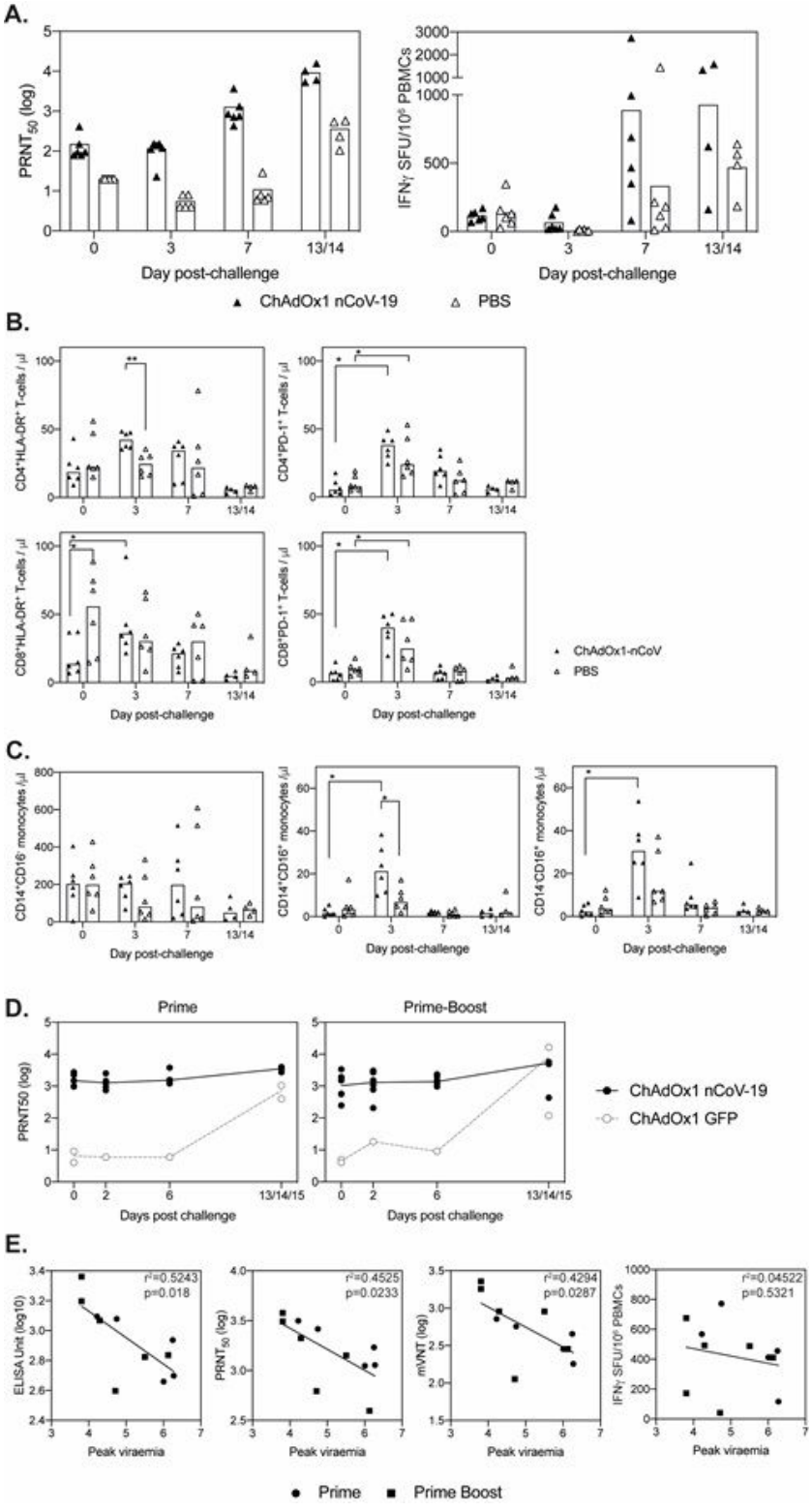


## Figure 5

Immune responses following challenge with SARS-CoV-2 a. Immune responses following challenge of rhesus macaques with SARS-CoV-2 was measured in virus neutralisation assays and by IFNγ ELISpot. b. Quantification of CD4+ and CD8+ T cells expressing HLA-DR and PD-1 prior to (day 0) and at days 3, 6-7 (7) and 13-14 post SARS-CoV-2 challenge of NHPs. c. Quantification of NHP monocyte sub-populations determined by expression of CD14 and CD16 by whole blood immunophenotyping flow cytometry assay.

Bars show group medians with values measured in individual animals shown. Asterisks denote significant differences determined by Wilcoxon signed rank test or Mann-Whitney U-test for paired and unpaired comparisons, (*) $p \leq 0.05$, ** $p \leq 0.01$. d. Antibody responses in ferrets following challenge was measured in virus neutralisation assay. e. To determine whether antibody responses impacted on protection of ferrets from SARS-CoV-2 infection, a Pearson correlation analysis was performed comparing peak viraemia in each ferret to IgG ELISA Unit, neutralisation titre (PRNT50), psuedoneutralisation titre (mVNT) or IFNγ ELISpot on the day of challenge, r2 and p values are indicated on each graph.

## Supplementary Files

This is a list of supplementary files associated with this preprint. Click to download.

- PHEpaperNatCommssuppinfofinal.docx
- NCOMMS2050697rs.pdf